

Development of pixelated scintillator-based compact radio-TLC

Sang June Jeon^a, Kyeong Min Kim^a, JongGuk Kim^{a*}

^aKorea Institute of Radiological and Medical Sciences, Seoul 01812, Rep. of Korea.

*Corresponding author: jgkim@kirams.re.kr

1. Introduction

Radio-TLC scanner, which is named after one of radio-detectors based on the technology of thin-layer chromatography, is generally the standard QC(Quality Control) equipment for analyzing the radiochemical purity in nuclear medicine[1][2]. The radio-TLC system generally shows as a graph of counting gamma radioactivity, emitting by radiopharmaceutical including a specific radioisotope. it makes guarantee quantitative accuracy and reproducibility for chemically stability and change of a targeting radiopharmaceutical.

In present the radio-TLC produced by a few companies use a gas-filled proportional counter with high cost, and it has limitations of both gas diffusion and ion density. Recently, Ce:GAGG has been developed and presented as promising scintillators for PET and SPECT due to high density, high light yield (~46,000~51,000 photon/MeV), and fast decay time[3][4]. We have adapted GAGG scintillation crystal array to radio-TLC detector.

2. Methods

2.1 Scintillation detector Model

The detection area for radio-TLC is 20 mm (W) × 100 mm (D). The detectors consist of GAGG crystal arrays and 0.8 mm(W) × 0.8 mm(H) × 128 pixels photodiode arrays.

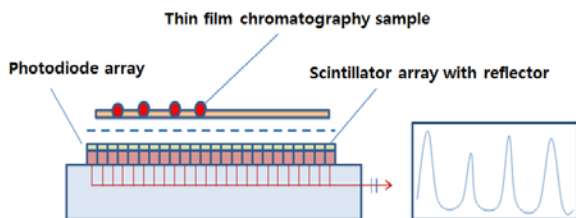


Fig. 1. Block diagram of Radio-TLC detector

The MCNPX Monte-Carlo simulation was conducted to investigate the optical photons created from in various sizes of GAGG crystal arrays, and incident optical photons into the photodiode pixel detector.

The GAGG crystal arrays, 0.6 mm(W) × 20 mm(D) × 1~5 mm(H) × 128 crystals, 1.4 mm(W) × 20 mm(D) × 1~5 mm(H) × 64 crystals, were modeled for simulation. Each crystal was polished and separated by 0.2 mm thickness of white reflectors.

The targeted performance of minimum sensitivity is about 1 $\mu\text{Ci}/\mu\text{l}$ with F-18 source. The radiation source used for the simulation was 1 μCi of F-18. The scintillator geometry is optimized using simulated data, absorption optical photons on the photodiode pixel, calculated spatial resolutions, and measured photodiode data. To determine crystal geometry, we compare the simulated results to the measured performance of 3 mm(W) × 20 mm(D) × 3 mm(H) GAGG crystal array.

2.2 Signal process and DAQ.

Fig. 2. Shows the block diagram of the electronics setup need for the readout of the detector. The photodiode arrays operate in order of two digital pulses; a clock pulse and a reset pulse. The clock pulse decides the signal charge integration time of each pixel, and the reset pulse decides the operation timing of start and end. We use 16-bit, 250 kS/s signal process system that consists of two channels of digital outputs and two channels of analog inputs. The two pair of output channels generates the clock and the reset pulses. The two input channels acquire the charge integration signal and triggering signal. The acquisition data is processed in the PC using Lab view software.

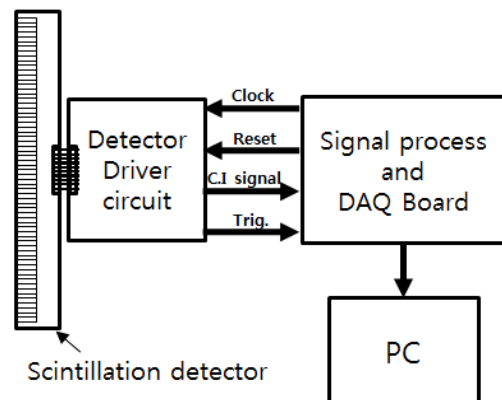


Fig. 2. The block diagram of used system to operating detector

2.3 Compact radio-TLC device

We developed and designed GAGG crystal based scintillation detector and electronic boards were used in the device shown fig.3, which is compact radio-TLC device RT-102. The RT-102 has the compact size of 166(W) x 142(D) x 71(H) mm. Fig.4 is the size comparing photo of RT-102 with the commonly used radio-TLC scanner(Bioscan AR-2000).

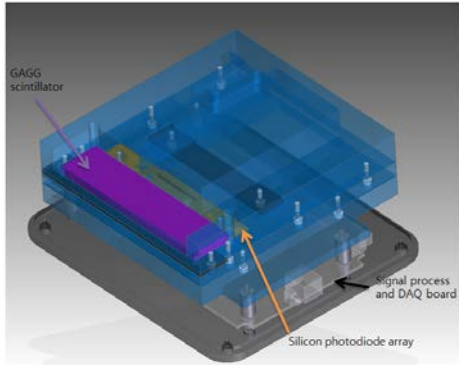


Fig. 3. The device structure of RT-102

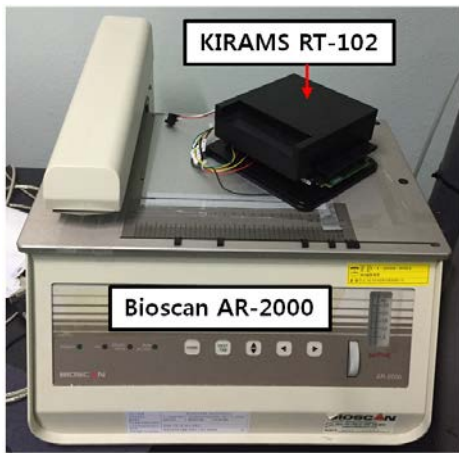


Fig. 4. Size comparison of RT-102 and AR-2000

2.4 performance test of RT-102

In order to test the performance of RT-102, we used $1\mu\text{Ci}/\mu\text{l}$ of Tc-99m and F-18 solutions. The points of radio-isotope (RI) solutions were spotted on $10 \times 100 \text{ mm}^2$ of cellulose fibers pressed paper. The volume of $1 \mu\text{l}$ RI solution was spotted at three points with equal distances.

We scanned each sample using RT-102 and AR-2000, and compared the ROI counts ratio and position data.

To compare the peak position, we calculated the distance ratio of each peaks.

3. Results

3.1 Simulation results of Scintillation detector

Fig. 5 shows the incidence optical photon on a photodiode pixel, which emitted from several sizes of GAGG crystal arrays. The black point is the measured data of $3(\text{W}) \times 20(\text{D}) \times 3\text{mm}(\text{H}) \times 33$ GAGG crystals array with $1 \mu\text{Ci}$ of F-18 source. The green and red points are simulated data of $0.6 \text{ mm}(\text{W}) \times 20 \text{ mm}(\text{D}) \times 1\sim 5 \text{ mm}(\text{H}) \times 128$ crystals array and $1.4 \text{ mm}(\text{W}) \times 20 \text{ mm}(\text{D}) \times 1\sim 5 \text{ mm}(\text{H}) \times 64$ crystals array. All the points of $0.6 \text{ mm}(\text{W})$ are lower than $3 \text{ mm}(\text{W})$ data.

Over 3 mm of height with $1.4 \text{ mm}(\text{W}) \times 20 \text{ mm}(\text{D})$ show enough intensity of optical photon.

The spatial resolution simulation data of crystal arrays are Fig. 6. The size of $1.4 \text{ mm}(\text{W}) \times 20 \text{ mm}(\text{D}) \times 3 \text{ mm}(\text{H})$ scintillator array has the best FWHM among $3\sim 5 \text{ mm}(\text{H})$ scintillator arrays.

We made scintillation detector using $1.4 \text{ mm}(\text{W}) \times 20 \text{ mm}(\text{D}) \times 3 \text{ mm}(\text{H}) \times 64$ pixels array and 128 channel photodiode.

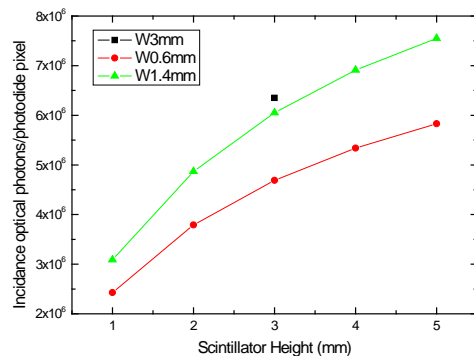


Fig. 5. The simulated data of incidence optical photon on a photodiode surface (red and green) and measured data (black dot).

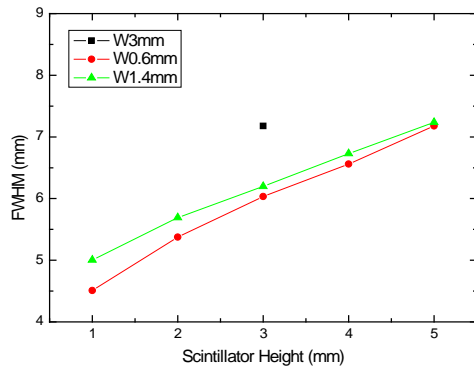


Fig. 6. The simulated spatial resolution data of GAGG crystal arrays

3.2 Performance test results of RT-102

The chromatogram scanning data of Tc-99m and F-18 spots are shown in Fig.7 and 8. The spatial resolution of RT-102 is poor compared to AR-2000, but it shows good ROI counts ratio and position of each peak.

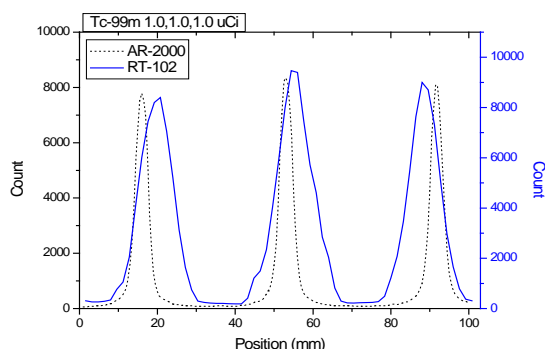


Fig. 7. The chromatogram scanning data of Tc-99m

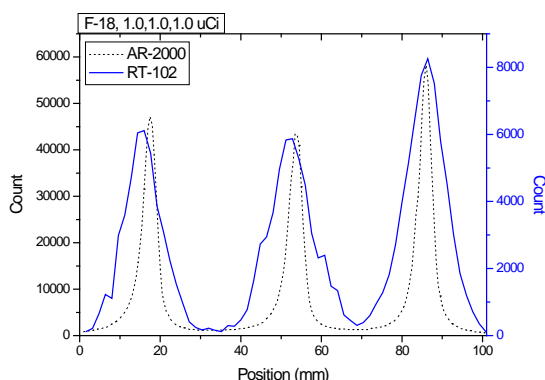


Fig. 8. The chromatogram scanning data of F-18

Table 1 is the calculated ROI counts ratio of each peak. The ROI count ratios differences between RT-102 and AR-2000 are less than 1.2%.

Each peak position and the calculated distance ratios are shown table 2. All of peak distance ratios are approximately equal to 1:1(0.96:1~1:1)

Table 1. ROI counts analysis data of Fig 7 and 8

Isotope	Device	% ROI		
		1 st	2 nd	3 rd
Tc-99m	AR-2000	32.1	35.0	32.9
	RT-102	31.3	36.2	32.5
F-18	AR-2000	32.2	30.4	37.5
	RT-102	31.1	31.8	38.1

Table 2. Peak position analysis data of Fig 7 and 8

Isotope	Device	Peak position (mm)			(2 nd -1 st) : (3 rd -2 nd)
		1 st	2 nd	3 rd	
Tc-99m	AR-2000	15.99	52.98	91.50	0.96 : 1
	RT-102	20.80	54.40	88.00	1 : 1
F-18	AR-2000	17.49	53.49	85.99	1.1 : 1
	RT-102	16.00	52.80	86.40	1.1 : 1

4. Conclusions

We developed the GAGG crystal array based radio-TLC RT-102. The RT-102 has several advantages such as the compact size, the no-gas usage, and the lower cost in comparison with commercial radio-TLC scanner.

In order to verify the performance of RT-102, we compared RT-102 with AR-2000. We scanned and compared Tc-99m and F-18 solution spotted samples in the same conditions. The ROI counts ratio and position detecting performances of RT-102 are approximately same with AR-2000. The results indicate the RT-102 has enough resolution and sensitivity to be used in the measurement of radiochemical purity test in radio-TLC devices.

REFERENCES

- [1] Peter F. Sharp, Howard G. Gemell and Alison D. Murray, Practical Nuclear Medicine 3rd edition, Springer, London, pp 131-135, 2005
- [2] Ilse Zolle, Technetium-99m Pharmaceuticals, Springer, Berlin, pp 123-135, 2007
- [3] A. Yochikawa, V. Chani and M. Nikl, Czochralski Growth and Properties of scintillating crystals, Acta. Phys. Pol. A, Vol.124, pp. 250-264, 2013
- [4] T. Yanagida, et al., Positive hysteresis of Ce-doped GAGG scintillator, Optical materials, Vol.36, pp.2016-2019, 2014